

Tests on Alkali-Activated Slag Foamed Concrete with Various Water-Binder Ratios and Substitution Levels of Fly Ash

Keun-Hyeok Yang^{1*}, Kyung-Ho Lee²

¹Department of Plant & Architectural Engineering, Kyonggi University, Suwon, Korea; ²Department of Architectural Engineering, Kyonggi University Graduate School, Seoul, Korea.

*Corresponding author: yangkh@kgu.ac.kr

Received February 16th, 2013; revised March 17th, 2013; accepted March 25th, 2013

ABSTRACT

To provide basic data for the reasonable mixing design of the alkali-activated (AA) foamed concrete as a thermal insulation material for a floor heating system, 9 concrete mixes with a targeted dry density less than 400 kg/m³ were tested. Ground granulated blast-furnace slag (GGBS) as a source material was activated by the following two types of alkali activators: 10% Ca(OH)₂ and 4% Mg(NO₃)₂, and 2.5% Ca(OH)₂ and 6.5% Na₂SiO₃. The main test parameters were water-to-binder (*W/B*) ratio and the substitution level (*R_{FA}*) of fly ash (FA) for GGBS. Test results revealed that the dry density of AA GGBS foamed concrete was independent of the *W/B* ratio and *R_{FA}*, whereas the compressive strength increased with the decrease in *W/B* ratio and with the increase in *R_{FA}* up to 15%, beyond which it decreased. With the increase in the *W/B* ratio, the amount of macro capillaries and artificial air pores increased, which resulted in the decrease of compressive strength. The magnitude of the environmental loads of the AA GGBS foamed concrete is independent of the *W/B* ratio and *R_{FA}*. The largest reduction percentage was found in the photochemical oxidation potential, being more than 99%. The reduction percentage was 87% - 93% for the global warming potential, 81% - 84% for abiotic depletion, 79% - 84% for acidification potential, 77% - 85% for eutrophication potential, and 73% - 83% for human toxicity potential. Ultimately, this study proved that the developed AA GGBS foamed concrete has a considerable promise as a sustainable construction material for nonstructural element.

Keywords: Alkali-Activated Foamed Concrete; Granulated Ground Blast-Furnace Slag; Fly Ash; Water-to-Binder Ratio; Environmental Load

1. Introduction

Most of residential buildings and houses in Korea adopt a floor heating system. The floor radiation heating system is commonly estimated to be lower as much as 50% in energy consumption compared with convection heating system [1]. Furthermore, the floor heating system can be converted to a floor cooling system by using a heat pump system. As a result, several countries have been recently interested in the floor heating system to overcome the limitation of convection heating system and enhance indoor environmental quality and comfort including energy conservation. In floor heating system, foamed concrete is commonly constructed between reinforced concrete slab and finishing mortar covering heating pipes to minimize a heat loss through concrete slab and to maintain the layout of heating pipe during construction of finishing mortar, as shown in **Figure 1**. Hence, foamed concrete for floor heating system fundamentally requires prefera-

bly lower density for lighter self-weight and lower thermal conductivity, while it also needs a minimum compressive strength at an early age to fix heating pipes and prevent its bearing failure during construction of heating pipe and finishing mortar.

In recent, various efforts have been attempted to reduce the use of ordinary Portland cement (OPC) for concrete production, because the OPC is generally estimated to be predominantly responsible for the environmental loads in the concrete industry [2,3]. One of the active alternatives for the OPC, an alkali-activated (AA) binder has begun to attract a great concern since the late 1980's, though further investigation and experimental verification on various essential performances including mechanical properties, inelastic behavior and durability need for the AA binder to practically apply to structural members. However, several reviews [4-8] reveal that the AA binder can draw a good strength gain property and beneficial environmental impact with low CO₂ emission

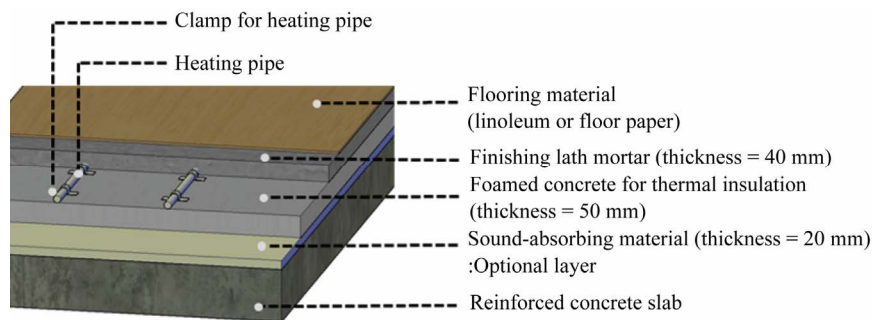


Figure 1. Typical section details of floor heating system.

and recycling of by-product materials such as ground granulated blast-furnace slag (GGBS) and fly ash (FA). Hence, AA binder would be considerable promise to produce a sustainable non-structural concrete element. Esmaily and Nuranian [9] showed that GGBS activated by sodium silicate solution can produce non-autoclaved high strength cellular concrete when the ratio of sodium silicate solution to aluminum powder for gas production is close to 1.0. Yang *et al.* [10] tested to develop AA GGBS foamed concrete as thermal insulation material for floor heating system and concluded that the unit binder content of approximately 400 kg/m^3 is required to achieve the minimum quality requirements specified in KS F 4039 [11] and ensuring the economic efficiency. On the other hand, the air-void system of foamed concrete, which significantly influences the strength and thermal conductivity of such concrete, depends on mixing proportions including water-to-binder ratio, foam volume and amount of filler as well as the performance of foam agent [12]. Furthermore, another current concern for the foamed concrete is sustainable quality. Therefore, various experiments and statistical data banks are required to establish a reliable mixing proportion for AA GGBS foamed concrete with a lower environmental impact.

The present experimental program was conducted as a follow-up to the previous investigation [10] to suggest a reasonable mixing proportion of AA GGBS foamed concrete for thermal insulation material in a floor heating system based on the various test data and understanding the behavior of such concrete. The main test parameters were water-to-binder (W/B) ratio and the substitution level (R_{FA}) of FA for GGBS. The quality and availability of the mixed foamed concrete were examined through comparisons with the minimum requirements (initial flow and defoamed depth for fresh concrete, and dry-density and compressive strength for hardened concrete) specified in KS F 4309 [11]. The effects of W/B ratio and RF on the characteristics of the air-void structure of the hardened concrete were ascertained by mercury intrusion porosimetry and light optical microscope. The environmental impacts of test mixes were also compared with

those calculated from a typical OPC foamed concrete mix.

2. Experimental Details

2.1. Specimens and Mixing Proportions

All specimens were classified into two groups according to the selected test parameters, as given in **Table 1**. The mixing details for specimens of Group I are as follows: water-to-binder (W/B) ratio as the main parameter varied from 40% to 50%; a combination of 10% $\text{Ca}(\text{OH})_2$ and 4% $\text{Mg}(\text{NO}_3)_2$ was used for an activator; and the unit binder content was fixed at 375 kg/m^3 . It is noted that the binder includes the source materials and activators. For specimens of Group II, FA was substituted for GGBS with the range of 0% - 20%, and then those source materials were activated by 2.5% $\text{Ca}(\text{OH})_2$ and 6.5% Na_2SiO_3 . The unit binder content and W/B ratio for mixes of Group II were fixed at 425 kg/m^3 and 37.5%, respectively. The foamed concrete for a floor heating system practically requires high workability with flow above 180 mm for self-compactability [1]. To achieve the high workability of all mixes, high early-strength agent containing water-reducing efficiency was added for mixes of Group I by 0.2% binder content, while 0.75% naphthalene-based high-range water-reducing agent was added for mixes of Group II. The foam volume required for a given unit binder content and W/B ratio was determined based on the procedure specified in ASTM C796-97 [13] together with the unit volume of concrete.

2.2. Materials

The chemical compositions of GGBS and FA obtained from x-ray fluorescence (XRF) analysis are given in **Table 2**. The GGBS was mainly composed of calcium, silicon, alumina and magnesium oxides. The FA used had a low calcium oxide (CaO) but was rich in both silicon and alumina as the silicon oxide (SiO_2)-to-aluminum oxide (Al_2O_3) ratio by mass is 1.91 which belongs to class F. The Blaine fineness and specific gravity were $4400 \text{ cm}^2/\text{g}$ and 2.9, respectively, for GGBS, and $4200 \text{ cm}^2/\text{g}$

Table 1. Mixing proportions of the foamed concrete specimens and summary of test results.

| Group | Specimens | Designed foam volume ratio (%) | W/B ratio (%) | R_{FA} (%) | Unit binder content (kg/m ³) | Composition of AA binder by weight (%) | | | | | Results of fresh concrete | | | Results of hardened concrete | | |
|-------|-----------|--------------------------------|---------------|--------------|--|--|----|-------------------------|--------------------------------------|---------------------------------------|------------------------------|-----------|---------------------|----------------------------------|---|------|
| | | | | | | GGBS | FA | Ca(OH) ₂ (%) | Na ₂ SiO ₃ (%) | Mg(NO ₃) ₂ (%) | Actual foam volume ratio (%) | Flow (mm) | Defoamed depth (mm) | Dry density (kg/m ³) | Compressive strength (MPa) 7 days 28 days | |
| I | I-40 | 71.24 | 40 | | | | | | | | 72.5 | ≥250 | 0 | 375 | 2.15 | 3.03 |
| | I-45 | 69.37 | 45 | 0 | 375 | 86 | - | 10 | - | 4 | 67.5 | ≥250 | 0 | 380 | 1.26 | 1.93 |
| | I-47.5 | 68.43 | 47.5 | | | | | | | | 67.1 | ≥250 | 0 | 391 | 1.06 | 1.63 |
| | I-50 | 67.49 | 50 | | | | | | | | 65.5 | ≥250 | 0 | 405 | 0.95 | 1.53 |
| II | II-0 | 69.00 | | 0 | | 91 | - | | | | 69.3 | 195 | 11 | 406 | 0.83 | 1.20 |
| | II-5 | 68.76 | | 5 | | 86 | 5 | | | | 68.1 | 200 | 12 | 409 | 0.97 | 1.68 |
| | II-10 | 68.53 | 37.5 | 10 | 425 | 81 | 10 | 2.5 | 6.5 | - | 67.8 | 215 | 14 | 403 | 1.54 | 2.16 |
| | II-15 | 68.30 | | 15 | | 76 | 15 | | | | 67.5 | 215 | 16 | 404 | 1.39 | 1.67 |
| | II-20 | 68.06 | | 20 | | 71 | 20 | | | | 67.8 | 220 | 17 | 405 | 0.87 | 1.30 |
| | | | | | | | | | | | | | | | | |

Note: In specimen notations, the first and second parts indicate the affiliated group and main parameter in each group, respectively. Hence, the second parts for Groups I and II refer to water-to-binder ratio and substitution level of FA for GGBS, respectively. For example, specimen I-40 indicates the foamed concrete mix with W/B ratio of 40% being affiliated to Group I, while specimen II-5 indicates the foamed concrete mix with R_{FA} of 5% being affiliated to Group II. *Concrete mixes of Group I contain high early-strength agent with water reducing efficiency by 0.2% binder content; **Concrete mixes of Group II contain 0.75% naphthalene-based high-range water-reducing admixture.

Table 2. Chemical composition of selected source materials (% by mass).

| Materials | SiO ₂ | Al ₂ O ₃ | Fe ₂ O ₃ | CaO | MgO | K ₂ O | Na ₂ O | TiO ₂ | SO ₃ | LOI* |
|-----------|------------------|--------------------------------|--------------------------------|-------|------|------------------|-------------------|------------------|-----------------|------|
| FA | 57.70 | 28.60 | 5.08 | 4.70 | 0.67 | 0.57 | 0.37 | 1.53 | 0.68 | 0.1 |
| GGBS | 34.70 | 13.80 | 0.11 | 44.60 | 4.38 | 0.48 | - | 0.74 | 0.95 | 0.24 |

*Loss on ignition.

and 2.2, respectively, for FA. All dry powdered alkali activators were pre-blended with source materials in the dry form. The specific gravity and maximum particle sizes were 2.24 and 21.2 mm, respectively, for Ca(OH)₂, 2.2 and 1026.1 mm, respectively, for Na₂SiO₃, 1.56 and 600 mm, respectively, for Mg(NO₃)₂. The foaming agent used to produce pre-foamed foam was a vegetable-based soap-type resin that is generally applied for OPC foamed concrete.

2.3. Mixing and Testing

All concrete specimens were produced in accordance with the pre-foamed foam mixing procedure recommended in ASTM C796-97 [13]. To produce foam, the foaming agent was diluted with water in the ratio of 1:19 by volume and then aerated to a density of 40 kg/m³ using a foam generator. The pre-formed foam was added to cementitious slurry and then mixed in a 0.12-m³ capacity circulating mixer pan.

For the fresh concrete, the initial flow tested without raising and dropping the flow table and defoamed depth were recorded in accordance with KS F 4039 [11]. The actual foam volume in the fresh concrete was also measured using a mess cylinder and methyl alcohol, with reference to the method proposed by Lee *et al.* [14]. The

compressive strength of concrete was measured using 100 × 200 mm cylinder at ages of 7 and 28 days. The dry density of hardened concrete was measured in accordance with KS F 2459 [11]. The pore size distribution and air-void structure were recorded at an age of 28 days by mercury intrusion porosimetry under pressures of 0 - 200 MPa, and by a light optical microscope, respectively. The inside of the steel molds to test the properties of hardened concrete were lined with stiff vinyl to prevent interaction with the mold release oil. Immediately after casting, most specimens were then sealed using a plastic bag to prevent evaporation and then cured at room temperature.

3. Test Results and Discussion

Test results are summarized in **Table 1**. As the foam content generally plays a leading factor in the foamed concrete with excessively low density [12], precisely controlling the designed foam volume being pumped into the cementitious slurry is essential to achieve the targeted properties of such concrete. However, an error between the actual foam content and designed value would be sometimes occurred because the density of pre-formed foam somewhat varies with the aerating time, pressure of compressed air connected with the foam generator and

atmospheric temperature. In the present test, the differences between the actual and the designed foam volumes were no more than 3%, indicating that the mixing and pumping of the pre-formed foam were successfully achieved as intended. Hence, the designed foam volume is used for the following discussion.

3.1. Flow of Fresh Concrete

All mixes showed the initial flow more than 180 mm, which is the minimum requirement value specified in KS F 4039 [11] (see **Table 3**). The value of initial flow of concrete mixes of Group I exceeded the diameter of table for measuring flow, though higher flow was visually observed with the increase in *W/B* ratio. The substitution of FA slightly contributed to improving the flow of AA GGBS foamed concrete, showing a higher flow with the increase in the substitution level (R_{FA}) of FA. The flow of fresh concrete demonstrates that the alkali activators selected for the present tests were effective in achieving high workability and preventing quick setting of the foamed concrete.

3.2. Defoamed Depth

The defoam in mixes of Group I almost did not occur, indicating that these specimens meet the requirement for Grade 0.6 of KS F 4039 [11]. On the contrary, Ca(OH)₂ and Na₂SiO₃-activated concrete mixes of Groups II showed relatively high defoamed depth. In particular, the defoamed depth increased with R_{FA} , indicating that the defoamed depth exceeded the minimum requirements for Grade 0.4 of KS F 4039 when the R_{FA} is above 15%. Severe defoam causes the deterioration of the thermal insulation capacity of the foamed concrete and cracking and settlement of the finishing lath mortar. From the comparison of activators used in Groups I and II, it can be inferred that Na₂SiO₃ as an activator is unfavorable to produce AA GGBS foamed concrete in terms of a burst of bubbles. The substitution of FA also accelerates the burst of bubbles in AA GGBS foamed concrete.

3.3. Dry Density

At the same unit binder content, the dry density of the

foamed concrete increased slightly with the *W/B* ratio owing to the decrease in foam content, as given in **Table 1**. The effect of replacement of FA on the dry density of AA GGBS foamed concrete was negligible, although the specific gravity of FA is lower than that of GGBS. The concrete mixes of Group I commonly met the density requirements of Grade 0.4 specified in KS F 4039, whereas those of Group II was relevant to Grade 0.5. Yang *et al.* [10] proposed that the dry density of the foamed concrete is proportional to its nominal unit weight ($W_n = W_B + W_W + W_f$) of the plastic mix based on absolute volume, where W_B , W_W , and W_f are the weights per unit volume of the binder, water and pre-foamed foam, respectively. The present tests also confirmed that the dry density of the AA GGBS foamed concrete can be expressed in terms of its nominal unit weight, as shown in **Figure 2**.

3.4. Compressive Strength

All concrete mixes achieved the minimum strength requirements of Grade 0.5 specified in KS F 4039. As might be expected, the compressive strength of the AA GGBS foamed concrete decreased with the increase in the *W/B* ratio, as given in **Table 1**. In general, concrete mixes in Group II developed lower strength than those in Group I. This indicates that 10% Ca(OH)₂ and 4% Mg(NO₃)₂ activators is more favorable than 2.5% Ca(OH)₂ and 6.5% Na₂SiO₃ activators in developing the compressive strength of AA GGBS concrete. The substitution of FA also significantly influenced the compressive strength of AA GGBS foamed concrete, showing that the compressive strength increased up to R_{FA} of 15%, beyond which it turned to decrease.

3.5. Porosity and Pore Structure

Figure 3 shows the effect of the *W/B* ratio on the pore size distribution of AA GGBS foamed concrete. It was fail to measure the pore size distribution in mixes of Group II. The air-void structure of mixes tested is also shown in **Figure 4**. The macro capillaries ($50 \leq \phi < 50 \mu\text{m}$) and artificial air pores ($50 \mu\text{m} \leq \phi$) result from the deliberately entrained air and insufficient compaction,

Table 3. Quality and grade of foamed concrete for thermal insulation specified in KS.

| Grade | Fresh concrete | | | | Hardened concrete | | |
|-------|--|-----------|---------------------|----------------------------------|----------------------------|---------|-----------------------------|
| | Wet density of slurry (kg/m ³) | Flow (mm) | Defoamed depth (mm) | Dry density (kg/m ³) | Compressive strength (MPa) | | Thermal conductivity (W/mK) |
| | | | | | 7 days | 28 days | |
| 0.4 | ≥390 | | ≤15 | 300 - 400 | ≥0.5 | ≥0.8 | ≤0.13 |
| 0.5 | ≥520 | ≥180 | ≤10 | 400 - 500 | ≥0.9 | ≥1.4 | ≤0.16 |
| 0.6 | ≥720 | | ≤6 | 500 - 700 | ≥1.5 | ≥2.0 | ≤0.19 |

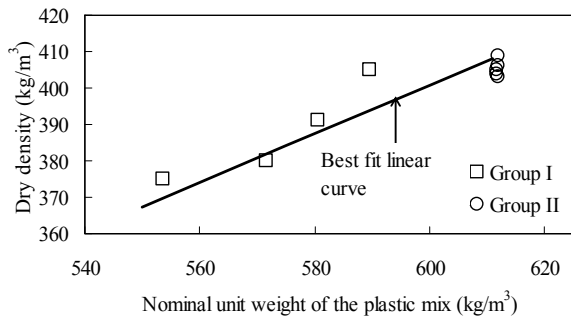


Figure 2. Relationship of nominal unit weight and dry density.

| Designation | W/B ration (%) | | | |
|---|----------------|-------|-------|-------|
| | 40 | 45 | 47.5 | 50 |
| Gel pores: $\phi < 10$ nm (%) | 0.89 | 1.03 | 0.97 | 1.54 |
| Micro capillaries: $10 \leq \phi < 50$ nm (%) | 14.85 | 12.99 | 11.51 | 10.47 |
| Micro capillaries: $50 \text{ nm} \leq \phi < 50 \mu\text{m}$ (%) | 32.05 | 34.54 | 36.21 | 41.56 |
| Artificial air pores: $50 \text{ nm} \leq \phi$ (%) | 7.45 | 8.17 | 8.84 | 9.91 |
| Total porosity (%) | 55.24 | 56.72 | 57.53 | 63.48 |

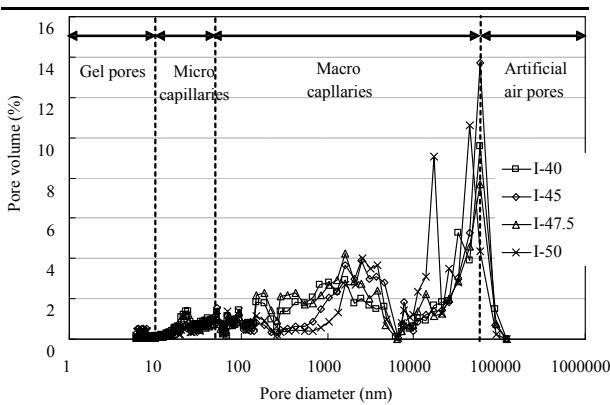


Figure 3. Effect of W/B ratio on the pore size distribution.

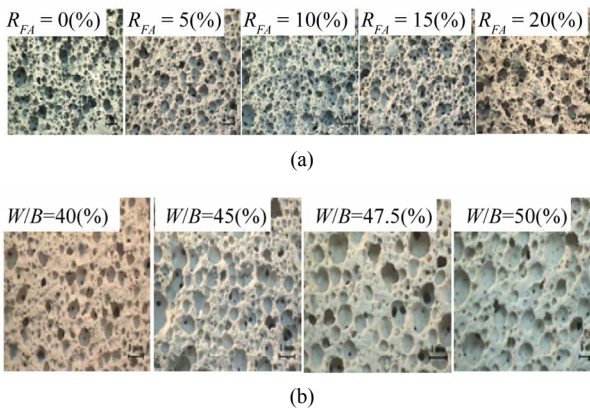


Figure 4. Air-void structure of AA GGBS foamed concrete. (a) Effect of R_{FA} ; (b) Effect of W/B .

where ϕ is the pore diameter. With the increase in the W/B ratio, the amount of micro capillaries decreased

whereas those of macro capillaries and artificial air pores increased, which resulted in the increase in porosity. In addition, a few bigger-sized pores were found, and their number also increased in concrete with higher W/B ratio. On the other hand, the amount of bigger-sized pores decreased with the increase in R_{FA} up to 10%, beyond which it increased. The effect of test parameters on pore size distribution and air-void structure of the foamed concrete was coincident with the observation in compressive strength. This indicates that the increase of macro capillaries and artificial air pores are responsible for reduction in strength.

4. Environmental Impact

The environmental loads of foamed concrete were calculated in accordance with the lifecycle assessment (LCA) procedure specified in ISO 14040 series [15] based on the Korean lifecycle inventory (LCI) database [16]. The studied boundary condition was from the cradle to the pre-construction system including various contributions that are subdivided into the constituent phase, production phase using a mixer in the construction site, and transportation phase from the gate of the raw material-producing facility to the site. The LCI for a building material provides a collective data set that covers everything from the cradle to the grave. The CO_2 inventory for the concrete production phase was obtained from the conversion of energy sources consumed in the mixer. The procedure and typical examples of LCA for various environmental loads are explained in detail in literature [17].

Table 4 summarizes the magnitude of the environmental loads determined from the mixing proportion of each specimen based on the LCA procedure. The environmental load inventories obtained from the typical OPC foamed concrete used for cost comparisons are also given for comparisons. The W/B ratio, unit binder content and designed foam volume ratio of OPC foamed concrete were typically assumed to be 50%, 425 kg/m^3 , and 65%, respectively, based on the case investigation result [1]. Because the CO_2 inventory of Na_2SiO_3 are considerably higher than those of $Ca(OH)_2$ and $Mg(NO_3)_2$, the CO_2 emission of concrete mixes of Group II was commonly higher than those of mixes of Group I. The magnitude of the environmental loads of the AA GGBS foamed concrete tested is independent of the W/B ratio and R_{FA} .

The magnitude of the environmental loads of the foamed concrete tended to be remained constant regardless of the W/B ratio and R_{FA} . This is because the unit binder content, which governs the environmental load of concrete, was fixed in each group. Among the environmental load measures in each AA GGBS mix, the largest was the CO_2 emission which was followed by the consumption of natural gas. The CO_2 emission of AA GGBS

Table 4. Environmental load inventories of each concrete mix calculated from LCA procedure.

| Specimen | Environmental load inventories (kg/m ³) | | | | | | | | |
|----------|---|----------|-----------------|-----------------|-----------------|--------------------|-----------------|-------------|-----------|
| | Emissions | | | | | Primary energy use | | | |
| | CO ₂ | CO | SO _x | NO _x | NH ₃ | Anthracite coal | Bituminous coal | Natural gas | Crude oil |
| I-40 | 3.18E+01 | 2.20E-02 | 3.45E-02 | 2.29E-01 | 3.62E-03 | 7.36E-01 | 4.04E-03 | 1.51E+01 | 2.44E+00 |
| I-45 | 3.18E+01 | 2.20E-02 | 3.45E-02 | 2.29E-01 | 3.62E-03 | 7.36E-01 | 4.04E-03 | 1.51E+01 | 2.44E+00 |
| I-47 | 3.18E+01 | 2.20E-02 | 3.45E-02 | 2.29E-01 | 3.62E-03 | 7.36E-01 | 4.04E-03 | 1.51E+01 | 2.44E+00 |
| I-50 | 3.18E+01 | 2.20E-02 | 3.45E-02 | 2.29E-01 | 3.62E-03 | 7.36E-01 | 4.04E-03 | 1.51E+01 | 2.44E+00 |
| II-F00 | 5.46E+01 | 2.97E-02 | 4.96E-02 | 1.56E-01 | 2.67E-03 | 2.10E-01 | 2.65E-03 | 8.91E+00 | 6.30E+00 |
| II-F05 | 5.44E+01 | 2.90E-02 | 4.95E-02 | 1.55E-01 | 2.67E-03 | 2.10E-01 | 2.59E-03 | 8.91E+00 | 6.30E+00 |
| II-F10 | 5.42E+01 | 2.83E-02 | 4.93E-02 | 1.54E-01 | 2.67E-03 | 2.10E-01 | 2.52E-03 | 8.91E+00 | 6.30E+00 |
| II-F15 | 5.40E+01 | 2.76E-02 | 4.91E-02 | 1.54E-01 | 2.67E-03 | 2.10E-01 | 2.46E-03 | 8.91E+00 | 6.30E+00 |
| II-F20 | 5.38E+01 | 2.68E-02 | 4.89E-02 | 1.53E-01 | 2.67E-03 | 2.10E-01 | 2.39E-03 | 8.91E+00 | 6.30E+00 |
| OPC | 4.43E+02 | 3.80E+01 | 2.54E-01 | 9.73E-01 | 6.29E-02 | 3.23E+00 | 7.66E+01 | 3.46E+00 | 1.35E+01 |

foamed concrete was evaluated to be considerably reduced by 93% for mixes of Group I, and 88% for mixes of Group II, compared with that of OPC foamed concrete. The reduction percentage of each environmental impact profile of AA GGBS foamed concrete relative to the typical OPC foamed concrete is plotted in **Figure 5**. The selected environmental impact category included abiotic depletion, global warming potential, acidification potential, eutrophication potential, photochemical oxidation potential, and human toxicity potential. The largest reduction percentage was found in the photochemical oxidation potential, being more than 99%. The reduction percentage was 87% - 93% for the global warming potential, 81% - 84% for abiotic depletion, 79% - 84% for acidification potential, 77% - 85% for eutrophication potential, and 73% - 83% for human toxicity potential. Overall, it can be concluded that the AA GGBS foamed concrete is promise as a sustainable building material with considerably reduced environmental impact.

5. Concluding Remarks

From the present experimental investigation and assessment of environmental impact, the following conclusions may be drawn:

- 1) The substitution of fly ash slightly contributed to improving the flow of AA GGBS foamed concrete.
- 2) Na₂SiO₃ as an activator is unfavorable to produce AA GGBS foamed concrete in terms of a burst of bubbles. The substitution of FA also accelerates the burst of bubbles in AA GGBS foamed concrete.
- 3) The dry density of the foamed concrete increased slightly with the *W/B* ratio, whereas the effect of replace-

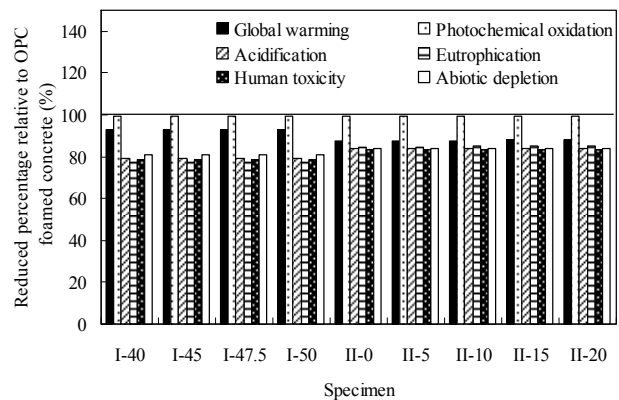


Figure 5. Reduction of each environmental impact profile of AA GGBS concrete relative to the typical OPC foamed concrete.

ment of fly ash on the dry density was negligible.

4) The compressive strength of the AA GGBS foamed concrete increased with the increase in *R_{FA}* up to 15%, beyond which it decreased.

5) With the increase in the *W/B* ratio, the amount of micro capillaries decreased whereas those of macro capillaries and artificial air pores increased, which resulted in the increase in porosity.

6) The magnitude of the environmental loads of the AA GGBS foamed concrete tested is independent of the *W/B* ratio and *R_{FA}*. The largest reduction percentage was found in the photochemical oxidation potential, being more than 99%. The reduction percentage was 87% - 93% for the global warming potential, 81% - 84% for abiotic depletion, 79% - 84% for acidification potential, 77% - 85% for eutrophication potential, and 73% - 83% for human toxicity potential.

6. Acknowledgements

This work was supported by the Basic Science Research Program through the National Research Foundation of Korea (NRF: 2009-0067189). The sponsor and technical participation of Hyundai Amco Co during the preparation of the test is greatly appreciated.

REFERENCES

- [1] J.-K. Song and K.-H. Yang, "Development of Environmental-Friendly High-Performance Floor System," Technical Report, Department of Architectural Engineering, Chonnam National University, Gwangju, 2012.
- [2] E. Gartner, "Industrially Interesting Approaches to 'Low-CO₂' Cements," *Cement and Concrete Research*, Vol. 34, No. 9, 2004, pp. 1489-1498.
[doi:10.1016/j.cemconres.2004.01.021](https://doi.org/10.1016/j.cemconres.2004.01.021)
- [3] B. L. Damineli, F. M. Kemeid, P. S. Aguiar and V. M. John, "Measuring the Eco-Efficiency of Cement Use," *Cement & Concrete Composite*, Vol. 32, No. 8, 2010, pp. 555-562. [doi:10.1016/j.cemconcomp.2010.07.009](https://doi.org/10.1016/j.cemconcomp.2010.07.009)
- [4] F. Pacheco-Torgal, J. Castro-Gomes and S. Jalali, "Alkali-Activated Binders: A Review-Part 1. Historical Background, Terminology, Reaction Mechanism and Hydration Products," *Construction and Building Materials*, Vol. 22, No. 7, 2008, pp. 1305-1314.
[doi:10.1016/j.conbuildmat.2007.10.015](https://doi.org/10.1016/j.conbuildmat.2007.10.015)
- [5] P. Duxson, A. Fernández-Jiménez, J. L. Provis, G. C. Lukey, A. Palomo and J. S. J. van Deventer, "Geopolymer Technology: The Current State of the Art," *Journal of Material Science*, Vol. 42, No. 9, 2007, pp. 2917-2933.
[doi:10.1007/s10853-006-0637-z](https://doi.org/10.1007/s10853-006-0637-z)
- [6] C. Shi, P. V. KrddShi and D. Roy, "Alkali-Activated Cements and Concretes," Taylor and Francis, London, 2006. [doi:10.4324/9780203390672](https://doi.org/10.4324/9780203390672)
- [7] S. D. Wang, X. C. Pu, K. L. Scrivener and P. L. Pratt, "Alkali-Activated Slag Cement and Concrete: A Review of Properties and Problems," *Advanced Cement Research*, Vol. 7, No. 27, 1995, pp. 93-102.
[doi:10.1680/adcr.1995.7.27.93](https://doi.org/10.1680/adcr.1995.7.27.93)
- [8] J. Davidovits, "Geopolymer: Chemistry & Applications," Géopolymère, 2008.
- [9] H. Esmaily and H. Nuranian, "Non-Autoclaved High Strength Cellular Concrete from Alkali Activated Slag," *Construction and Building Materials*, Vol. 26, No. 1, 2012, pp. 200-206.
[doi:10.1016/j.conbuildmat.2011.06.010](https://doi.org/10.1016/j.conbuildmat.2011.06.010)
- [10] K.-H. Yang, K.-H. Lee, J.-K. Song and M.-H. Gong, "Development of Alkali-Activated Slag Foamed Concrete for Thermal Insulation," *Cement & Concrete Composite*, Submitted for Publication, 2013.
- [11] KS F 2459, F 4039, "Korean Industrial Standard: Testing Concrete," Korean Standards Information Center (KS), Seoul (in Korean), 2006.
- [12] K. Ramamurthy, E. K. K. Nambiar and G. I. S. Ranjani, "A Classification of Studies on Properties of Foam Concrete," *Cement & Concrete Composite*, Vol. 31, No. 6, 2009, pp. 388-396.
[doi:10.1016/j.cemconcomp.2009.04.006](https://doi.org/10.1016/j.cemconcomp.2009.04.006)
- [13] ASTM C796-97, "Annual Book of ASTM Standards: V. 4.02," ASTM International, 2012.
- [14] D.-H. Lee, M.-H. Jun and J.-S. Ko, "Physical Properties and Quality Control of Foamed Concrete with Fly Ash for Cast-in-Site," *Journal of Korea Concrete Institute*, Vol. 13, No. 1, 2001, pp. 69-76 (in Korean).
- [15] ISO 14040, "Environmental Management-Life Cycle Assessment—Principles and Framework," International Standardisation Organisation 2006.
- [16] Korea LCI Database Information Network, (in Korean). <http://www.edp.or.kr/lcidb>
- [17] K.-H. Yang, J.-K. Song and K.-I. Song, "Assessment of CO₂ Reduction of Alkali-Activated Concrete," *Journal of Cleaner Production*, Vol. 39, No. 1, 2013, pp. 265-272.
[doi:10.1016/j.jclepro.2012.08.001](https://doi.org/10.1016/j.jclepro.2012.08.001)